Three-dimensional illumination analysis using wave equation based propagator

Xiao-Bi Xie IGPP, University of California, Santa Cruz, Shengwen Jin, Screen Imaging Technology Inc., and Ru-Shan Wu, IGPP, University of California, Santa Cruz*

Summary

A wave-equation based method is developed for seismic illumination analysis. The approach uses the one-way screen propagator to provide fast and accurate wavefield extrapolation. A local plane wave analysis is used to determine energy propagation directions. The method can avoid the singularity problem usually linked to the high frequency asymptotic method. It provides a practical tool for three-dimensional full-volume illumination analysis in complicated structures. To demonstrate the potential application of this method, numerical examples for the 3D SEG/EAGE salt model are calculated.

Introduction

Advances in seismic technology, particularly in prestack depth migration, have made significant improvement in providing reliable high-resolution images for complex structures. However, there is still a need to better understand how various factors affect image qualities. The seismic illumination analysis is a useful estimate that gives potential detecting power of a specific acquisition system for a given structure. Traditionally, illumination analysis is based on the ray tracing technique (Schneider, 1999; Bear et al., 2000; Muerdter et al., 2001abc). The ray-based methods can provide both the intensity and direction information carried in the wavefield. However, the high frequency asymptotic approximation and the singularity problem of the ray theory may severely limit its accuracy in complex regions (Hoffmann, 2001). Full-wave finite-difference method is widely used for wave propagation simulation. However, for illumination analysis purpose, it usually provides only the total illumination. The directional information of the wave propagation is lost. Finite-difference simulation is also expensive, which prohibits it from practical application for illumination analysis.

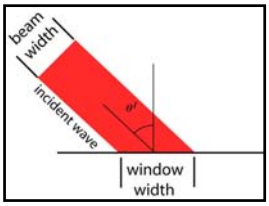

Figure 1. Basic angle domain information.

The recently developed dual-domain one-way wave equation based methods (e.g., Stoffa et al., 1990; Ristow and Ruhl, 1994; Jin, et al., 1998, 2002; Xie and Wu, 1998; Huang and Fehler, 2000; Xie et al., 2000; Wu and Chen, 2001; Biondi, 2002) provided accurate propagators for seismic wave extrapolation. To apply these propagators to illumination analysis, the central part is extracting angle related information from the propagated wavefield. To do this, Wu and Chen (2002) used the wavelet transform theory to decompose the wavefield into beamlets, which are localized in both space and directions, and successfully applied it to the illumination analysis. Xie and Wu (2002) proposed another approach based on the local plane wave analysis. In this research, we developed an illumination analysis method based on generalized screen propagator (Jin, et al., 1998; Xie and Wu, 1998) and the local plane wave analysis (Xie and Wu, 2002). Using this method, the seismic energy from the sources and receivers are propagated to the target region with a one-way wave equation based propagator. Then, a local plane wave analysis is conducted and directional energy fluxes are obtained from wavefields. By properly sorting energy fluxes in the target region, the total illumination, directional illumination, total dip-response and directional dip-response can be obtained.

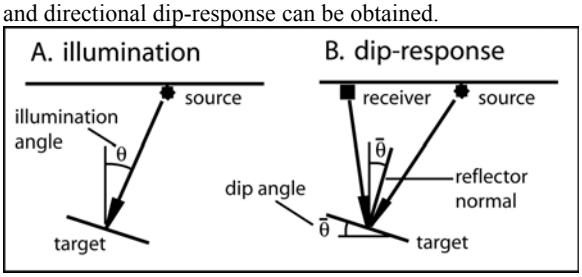

Figure 2. A sketch showing (a) the directional illumination and (b) the acquisition dip-response.

In the following sections, we first give a brief description on how to calculate the directional energy fluxes from the wavefield and apply them to the illumination analysis. Then, to demonstrate the potential applications of this method, illumination examples are calculated using the 3D SEG/EAGE Salt model. The results from the illumination analysis are compared with the prestack depth image obtained from the same model.

Angle domain analysis for extrapolated wavefields

Xie and Wu (2002) proposed an approach to extract angle related information from the wavefield using a local plane wave analysis. Figure 1 is a sketch showing the geometry of angle domain analysis. Using this method, the seismic energy from the sources or receivers is propagated to the target region with a wave equation based propagator. Then, a windowed Fourier transform is used to decompose the wavefield into localized plane waves

$$u(\mathbf{r}_S;\mathbf{x}_T,z,\mathbf{K}_T,\omega) = F\left[w(\mathbf{x}_T,\mathbf{x}'_T)u\ (\mathbf{r}_S;\mathbf{x}'_T,z,\omega)\right], \qquad (1)$$

where $u(\mathbf{r}_S;\mathbf{x}'_T,z,\omega)$ is the incoming wave, $\mathbf{r} = (\mathbf{x}_T,z)$ is the location, $\mathbf{x}_T$ is the horizontal location, z is the depth, $\mathbf{r}_S$

is the source location, $u(\mathbf{r}_S;\mathbf{x}_T,z,\mathbf{K}_T,\omega)$ is the local plane wave, w is a 2D window in the horizontal direction $\mathbf{x}'_T$ and centered at $\mathbf{x}_T$, $\mathbf{K}_T$ is the local horizontal wavenumber, $F[\cdot]$ is a 2D Fourier transform. A finite-sized window is required for local plane wave analysis under finite frequencies. The size of the window provides the trade off between the spatial and angle resolutions. The local horizontal wavenumber $\mathbf{K}_T$ can be transformed to angle $\boldsymbol{\theta}=(\theta,\varphi)$, where $\theta(\mathbf{K}_T)=\sin^{-1}(K_T/k)$ and $\varphi(\mathbf{K}_T)=\tan^{-1}(K_Y/K_X)$, $k=\omega/\alpha$ is the local wavenumber and α is the local velocity. The local plane wave can also be written as $u(\mathbf{r}_S;\mathbf{x}_T,z,\boldsymbol{\theta},\omega)$.

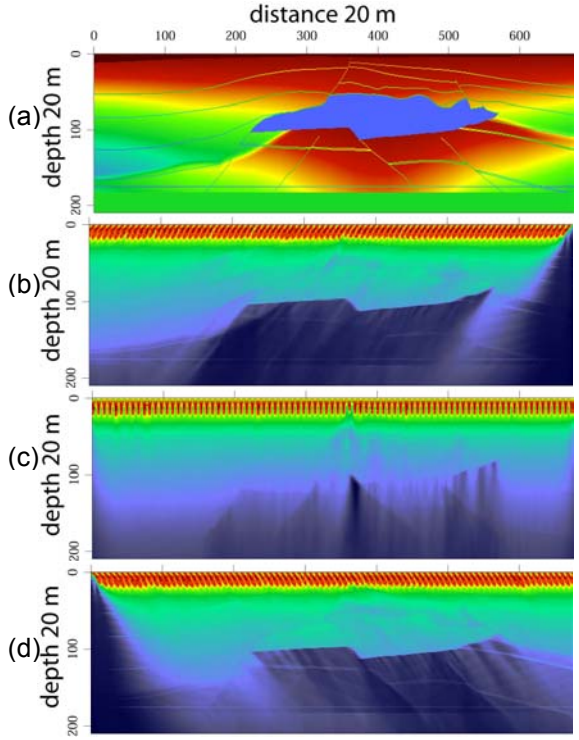

Figure 3. DI maps for the 3D SEG/EAGE salt model. Shown in the figure are cross sections at y = 6100 m, with (a) velocity model, (b) DI of 45˚ left, (c) vertical DI, and (d) DI of 45˚ right.

Illumination analysis and dip-response analysis

An illumination is the energy flux at the target generated by the seismic source (see Figure 2a). The illumination can be described with the intensity and direction of the incoming energy

$$I(\mathbf{r}_S;\,\mathbf{x}_T,z,\boldsymbol{\theta},\omega) = u(\mathbf{r}_S;\mathbf{x}_T,z,\boldsymbol{\theta},\omega)\cdot u^*(\mathbf{r}_S;\mathbf{x}_T,z,\boldsymbol{\theta},\omega) \quad (2)$$

where I is called directional illumination (DI), "*" denotes complex conjugate. For an acquisition system composed of multiple sources, their combined illumination can be obtained by summing up energy from the individual sources

$$I(\mathbf{x}_T,z,\boldsymbol{\theta},\omega)=\sum_{\mathbf{r}_S} I(\mathbf{r}_S;\mathbf{x}_T,z,\boldsymbol{\theta},\omega)\ . \quad (3)$$

DI can be further sorted according to different purposes to give useful information. For example, the total illumination can be obtained by summing up energy fluxes from all directions. The result can also be summed up over the frequency ω.

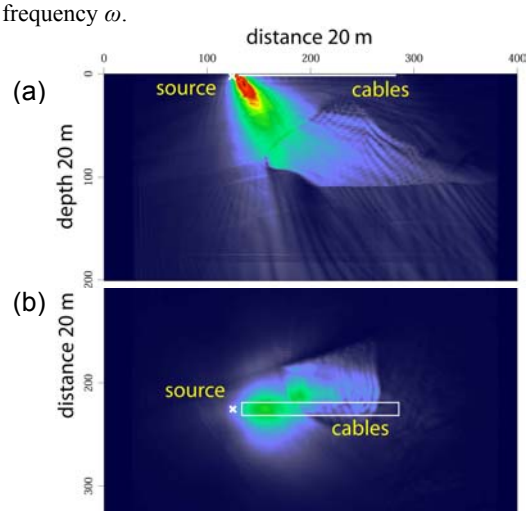

Figure 4. The ADR from a single shot in a 3D model. The dip angle is 30˚. Shown in (a) is the vertical profile, (b) is the depth slice at z = 1000 m. The acquisition system composed of a source and four 3200 m cables, which have been marked in the figure.

The acquisition dip-response (ADR) is a simulation of the detecting power of a source-receiver pair (see Figure 1B), which can be expressed as

$$R(\mathbf{r}_S;\mathbf{r}_R;\mathbf{x}_T,z,\bar{\boldsymbol{\theta}},\omega) = \left[I(\mathbf{r}_S;\mathbf{x}_T,z,\boldsymbol{\theta}_S,\omega)\cdot I(\mathbf{r}_R;\mathbf{x}_T,z,\boldsymbol{\theta}_R,\omega)\right]^{1/2} \quad (4)$$

where $\mathbf{r}_R$ is the location of the receiver, $I(\mathbf{r}_S)$ and $I(\mathbf{r}_R)$ are DIs from the source and receiver, $\boldsymbol{\theta}_S$ and $\boldsymbol{\theta}_R$ are their illumination angles, $\bar{\boldsymbol{\theta}}$ is the angle bisector of $\boldsymbol{\theta}_S$ and $\boldsymbol{\theta}_R$, which is also the dipping angle of the favorite reflector. The energy fluxes are calculated from both source and receiver to the target. According to the seismic representation reciprocity, the later is equivalent to the up-going energy flux from the target to the receiver. Combining both energy fluxes together equivalents to a source-reflector-receiver process with a unit reflectivity. Its strength gives the detecting power of a specific source-receiver pair to the target in case there is a reflector. The most favorite structures that can be detected are those with their normal vectors parallel to the angle bisector of source and receiver side incoming fluxes. For an acquisition

system composed of multiple source-receiver pairs, its detecting power can be obtained by summing up contributions from individual source-receiver pairs according to the specific acquisition geometry, (e.g., multiple shots, cable length, sail direction, etc.)

$$R(\mathbf{x}_T, z, \overline{\boldsymbol{\theta}}, \omega) = \sum_{\mathbf{r}_S} \sum_{\mathbf{r}_R} R(\mathbf{r}_S; \mathbf{r}_R; \mathbf{x}_T, z, \overline{\boldsymbol{\theta}}, \omega). \quad (5)$$

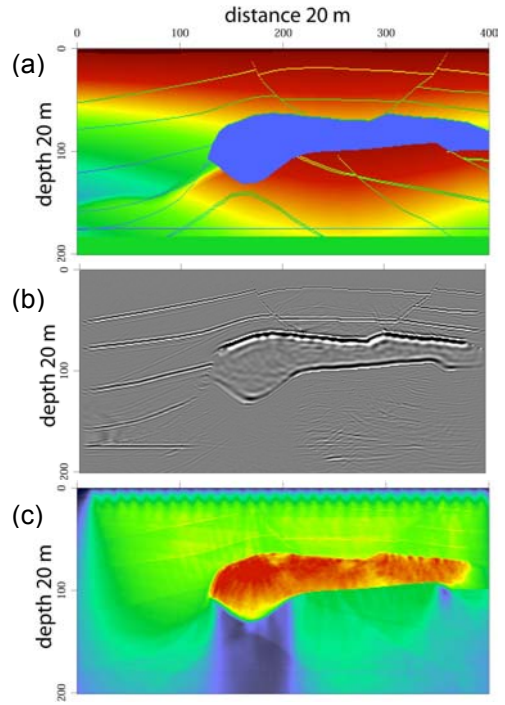

Figure 5. ADRs for the 3D SEG/EAGE salt model. Shown in the figure are cross sections at y = 2440 m, with (a) velocity model, (b) prestack depth image and (c) vertical ADR.

Numerical examples

To demonstrate the application of the illumination analysis, we calculated a number of numerical examples using the 3D SEG/EAGE velocity model. Shown in Figure 3 are DI (directional illumination) maps in a cross section at y = 6100 m, with (a) velocity model, (b) 45˚ DI towards left, (c) vertical DI, and (d) 45˚ DI towards right. About 3600 sources are used to illuminate the model. The results clearly show that the high velocity salt body effectively blocks the energy from reaching to the subsalt region. It is especially difficult for obliquely propagated energy to penetrate the salt body, which makes imaging the subsalt steep structures a challenge.

Shown in Figure 4 is a 30˚ ADR (acquisition dip-response) from a single shot and four 3200 m long cables in the 3D SEG/EAGE salt model. The locations of the source and cables are indicated in the figure. These ADR maps reveal the relationship between the detecting power, the specific source-cable system and the complex velocity model. Figure 5 gives the ADR for the SEG/EAGE model at y = 2440 m, with (a) velocity model, (b) prestack depth image,

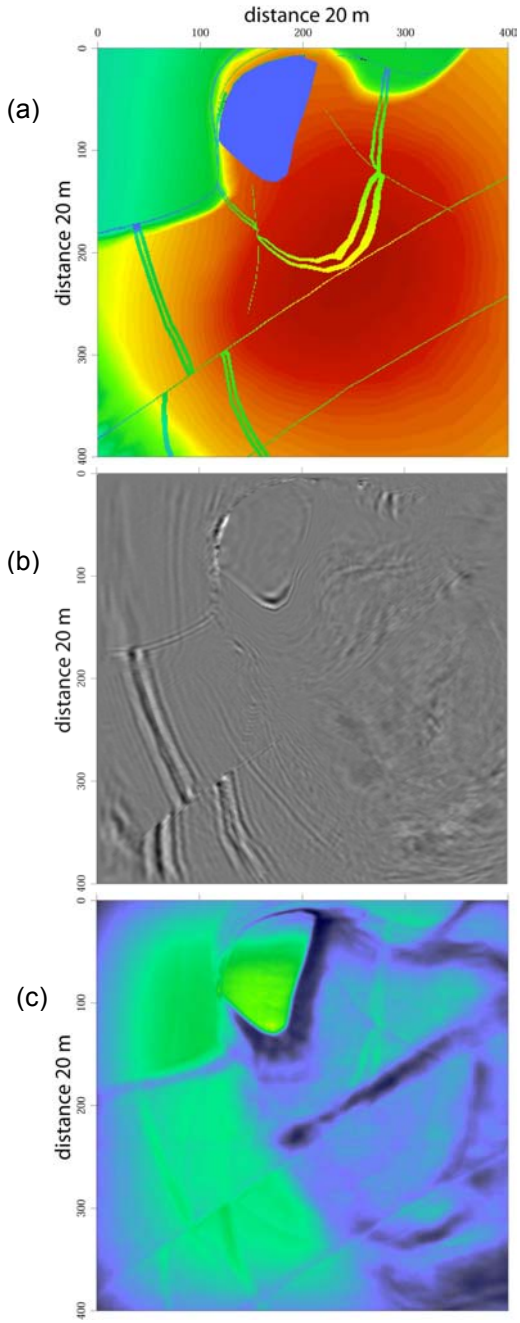

Figure 6. ADRs for the 3D SEG/EAGE salt model. Shown in the figure are depth slices at z = 2500 m, with (a) velocity model, (b) prestack depth image and (c) total ADR.

and (c) the vertical ADR. About 500 surface shots are used to illuminate the model. In the vertical ADR, a shadow zone can be seen beneath the salt body. This shadow zone is consistent with the depth image where the subsalt structures, including the horizontal base line, are totally missing. Figure 6 gives similar results for the total ADR. Shown in the figure are depth slices at z = 2500 m. In Figure 6b, the prestack depth image shows good quality on the left side, but the result is unsatisfied on the right side. The poor image quality can be explained with the low illumination region shown in Figure 6c.

Conclusions

A wave equation based method is developed for the illumination analysis. DI (directional illumination) and ADR (acquisition dip-response) maps can be extracted from the analysis. Using a dual-domain screen propagator, the approach is both fast and accurate. It provides a practical way to conduct 3D full-volume illumination analysis in complex structures. The results can either be used for the quality control in seismic migration, or be used to optimize the survey design. To demonstrate the capability of the method, the 3D full-volume DI and the ADR are calculated for the SEG/EAGE salt model. The resulted illumination maps are compared to the 3D prestack depth migration image from the same model. The illumination analysis properly reveals that the poor illumination condition is responsible for the unsatisfied image qualities in some subsalt regions. Although numerical examples provided in this paper is for marine type acquisitions with sources and receivers located on the same level, this method can also be used to simulate illuminations for ocean bottom cable or vertical cable geometry where sources and receivers are located at different depths. As a wave-equation based method, this approach can be naturally teamed with the wave-equation based migration algorithms for illumination analysis.

Acknowledgment

The research is supported by the DOE/BES Project at the University of California, Santa Cruz.

References

Bear, G., Lu, C., Lu, R. and Willen, D., 2000, The construction of subsurface illumination and amplitude maps via ray tracing, The Leading Edge, **19**(7), 726-728.

Biondi, B., 2002, Stable wide-angle Fourier finite-difference downward extraolation of 3-D wavefields, Geophysics, **67**, 872-882.

Hoffmann, J., 2001, Illumination, resolution, and image quality of PP- and PS-waves for survey planning, The Leading Edge, **20**(9), 1008-1014.

Huang, L.J. and Fehler, M.C., 2000, Globally optimized Fourier finite-difference migration method, Expanded Abstracts, SEG 70th Annual Meeting, 802-805.

Jin, S., and Wu, R. S., 1999, Common offset pseudo-screen depth migration, Annual Internat. Mtg., Soc. Expl. Geophys., Expanded Abstracts, 1516-1519.

Jin, S., Wu, R.S. and Peng, C., 1998, Prestack depth migration using a hybrid pseudo-screen propagator, Expanded Abstracts, SEG 68th Annual Meeting, 1819-1822.

Jin, S., Mosher, C.C., and Wu, R.S., 2002, Offset-domain pseudoscreen prestack depth migration: Geophysics, **67**, 1895-1902.

Muerdter, D. and Ratcliff, D., 2001a, Understanding subsalt illumination through ray-trace modeling, Part 1: Simple 2-D salt models, The Leading Edge, **20**(6), 578-594.

Muerdter, D., Kelly, M. and Ratcliff, D., 2001b, Understanding subsalt illumination through ray-trace modeling, Part 2: Dipping salt bodies, salt peaks, and nonreciprocity of subsalt amplitude response, The Leading Edge, **20**(7), 688-697.

Muerdter, D. and Ratcliff, D., 2001c, Understanding subsalt illumination through ray-trace modeling, Part 3: Salt ridges and furrows, and the impact of acquisition orientation, The Leading Edge, **20**(8), 803-816.

Ristow, D. and Ruhl, T, 1994, Fourier finite-difference migration, Geophysics, 59, 1882-1893.

Stoffa, P.L., Fokkema, J.T., Freire, R.M.D., and Kessinger, W.P., 1990. Split-step Fourier migration, Geophysics, **55**, 410-421.

Schneider, W.A. and Winbow, G.A., 1999, Efficient and accurate modeling of 3-D seismic illumination, 69th Ann. Internat. Mtg., Soc. Expl. Geophys., Expanded Abstracts, 633-636.

Wu, R.S. and Chen, L, 2001, Beamlet migration using Gabor-Daubechies frame propagator, 63rd Conference & Technical Exhibition, EAGE, Expanded abstracts, 74.

Wu, R.S. and Chen, L, 2002, Mapping directional illumination and acquisition-aperture efficacy by beamlet propagators, Annual Internat. Mtg., Soc. Expl. Geophys., Expanded Abstracts, 1352-1355.

Xie, X.B., Mosher, C.C. and Wu, R.S., 2000, The application of wide angle screen propagator to 2D and 3D depth migrations, Expanded Abstracts, SEG 70th Annual Meeting, 878-881.

Xie, X.B. and Wu, R.S., 1998, Improve the wide angle accuracy of screen method under large contrast, Expanded Abstracts, SEG 68th Annual Meeting, 1247-1250.

Xie, X.B. and Wu, R.S., 2002, Extracting angle domain information from migrated wavefield, Expanded Abstracts, SEG 72th Annual Meeting, 1360-1363.